



1 **Using Eddy Covariance Observations to Determine the Carbon**
2 **Sequestration Characteristics of Subalpine Forests in the Qinghai-**
3 **Tibet Plateau**

4 Niu Zhu^{1,2,4}, Jinniu Wang^{1,2}, Dongliang Luo³, Xufeng Wang³, Cheng Shen^{1,2}, Ning Wu¹

5 1 Chengdu Institute of Biology, Chinese Academy of Science, Chengdu 610041,
6 China

7 2 Mangkang Ecological Monitoring Station, Tibet Ecological Security Barrier
8 Ecological Monitoring Network, Qamdo 854500, China

9 3 Northwest Institute of Eco-environmental Resources, Chinese Academy of
10 Sciences, Lanzhou 730000, China

11 4 College of Resources and Environmental Sciences, Gansu Agricultural University,
12 Lanzhou 730070, China

13 **Correspondence:** Jinniu Wang (wangjn@cib.ac.cn)



14 **Abstract:** The subalpine forests in the Qinghai-Tibet Plateau (QTP) act as carbon sinks in the
15 context of climate change and ecosystem dynamics. In this study, we investigated the carbon
16 sequestration function using the *in-situ* observations from an eddy covariance system for the
17 subalpine forests. With two-year contiguous observations, the factors driving the seasonal variations
18 in carbon sequestration potential were quantified. We first revealed the seasonal characteristics of
19 carbon dynamics in the subalpine forests during the growing and dormant seasons, respectively. The
20 diurnal carbon exchange exhibited significant fluctuations, as high as $10.78 \mu\text{mol CO}_2 \text{ s}^{-1} \text{ m}^{-2}$ (12:30,
21 autumn). The period from summer to autumn was identified as the peak in carbon sequestration rate
22 in the subalpine forests. Subsequently, we explored the climatic factors influencing the carbon
23 sequestration function. Photosynthetically active radiation (PAR) was found to be a major climatic
24 factor driving the net ecosystem exchange (NEE) within the same season, significantly influencing
25 forest growth and carbon absorption. Increasing altitude negatively impacts carbon absorption at the
26 regional scale and the rising annual temperature significantly enhances carbon uptake, while the
27 average annual precipitation shows a minor effect on NEE. At the annual scale, the observations at
28 the subalpine forests demonstrated a strong carbon sequestration capability, with an average NEE
29 of $389.03 \text{ g C m}^{-2}$. Furthermore, we roughly assessed the carbon sequestration status of subalpine
30 forests in the QTP. Despite challenges caused by climate change, these forests possess enormous
31 carbon sequestration potential. Currently, they represent the most robust carbon sequestration
32 ecosystem in the QTP. We conclude that enhancing the protection and management of subalpine
33 forests under future climate change scenarios will positively impact global carbon cycling and
34 contribute to climate change mitigation. Moreover, this study provides essential insights for
35 understanding the carbon cycling mechanism in plateau ecosystems and global carbon balance.

36 **Keywords:** Subalpine forest; Qinghai-Tibet Plateau; The eddy covariance system; Three Parallel
37 Rivers Region; Carbon sinks

38 **1 Introduction**

39 Carbon dioxide (CO_2) is a prominent greenhouse gas, and its atmospheric concentration has
40 reached an unprecedented level in recent years, with a recorded peak of 419 parts per million (ppm).
41 Extensive research conducted by numerous scholars has consistently demonstrated that human
42 activities have been the primary catalyst behind the significant surge in atmospheric CO_2



43 concentrations since the 18th century (Stein, 2021). CO₂ and CH₄ collectively contribute
44 approximately 70% to the global warming potential among the six greenhouse gases specified in
45 the Kyoto Protocol (Zhang et al., 2022). As atmospheric CO₂ concentrations continue to rise, global
46 climate warming is gradually intensifying. Therefore, The Paris Agreement urges national
47 governments to restrict the increase in global average temperature to well below 2.0 °C above pre-
48 industrial levels and to strive to limit it to 1.5 °C. The increasing atmospheric CO₂ levels will lead
49 to irreversible ecological disasters. For instance, if global consumption of fossil fuels continues to
50 rise at the current rate, the concentration of CO₂ in the atmosphere is projected to double within
51 approximately 50 years. The rise in temperatures at 80 °S latitude could result in the melting of
52 glaciers, leading to a sea-level rise of 5 m (Mercer, 1978). By the year 2040, most countries are
53 projected to experience at least one annual disaster with a 50% or higher probability (Fortunato et
54 al., 2022). Addressing the greenhouse effect caused by carbon dioxide and reducing its impact is a
55 crucial challenge facing human society today. Reducing regional carbon emissions or per capita
56 carbon emissions is widely regarded as an effective approach to carbon reduction (Wang et al.,
57 2023a). Nevertheless, countries around the world have already begun to commit to carbon reduction
58 and carbon neutrality efforts. On September 22, 2020, during the 75th session of the United Nations
59 General Assembly, the Chinese government announced "double carbon" goals, which aims to
60 achieve carbon emission peaking by 2030 and carbon neutrality by 2060, in alignment with
61 ecological conservation and sustainable development objectives (Yu, 2022). It is predicted that
62 China's average forest carbon sequestration rate would reach to 0.358 Pg C year⁻¹ (petagrams of
63 carbon per year) by 2060 (Cai et al., 2022). This significant rate of carbon sequestration is expected
64 to have a substantial impact on the environment and economy, providing negative feedback to global
65 warming (Pan et al., 2011).

66 Forests cover approximately 30% of the earth's land surface and store around 90% of the
67 terrestrial vegetation carbon (Le Quéré et al., 2018). However, currently, there is no method
68 available to accurately quantify the carbon sequestration potential of forests. Quantitative estimation
69 of carbon sequestration potential still requires scientists to establish more *in-situ* sites and generate
70 comprehensive datasets to assess a wide range of area. Initially, individuals' biomass measurements
71 were used to estimate forest carbon sequestration capacity (Ebermayer, 1876). However, this



72 method was time-consuming, labor-intensive, and prone to inaccuracies due to the omission of
73 various variables during the calculation process. The development of modeling techniques allowed
74 for the use of simulation methods - forest management models and land ecosystem-climate
75 interaction models, such as the Ecological Assimilation of Land and Climate Observation (EALCO),
76 have been widely applied in this regard (Landsberg and Waring, 1997; Wang et al., 2001). Currently,
77 remote sensing monitoring and the eddy covariance method are widely used. Remote sensing
78 techniques can be used to extract vegetation parameters (such as NDVI) from multispectral bands
79 and estimate the carbon sequestration of entire forests through regression analysis (Laurin et al.,
80 2014). The theoretical foundation of the eddy covariance method was initially proposed by Swinbank
81 et al., (Swinbank, 1951). It started to be applied in carbon flux studies of forest ecosystems in the
82 1980s (Anderson et al., 1984). Nowadays, this method not only accurately measures the carbon
83 exchange between forests and the atmosphere but also integrates other instruments to measure
84 meteorological variables such as light intensity and temperature. It allows for long-term and
85 continuous calculation of carbon flux between forests and the atmosphere. Additionally, it provides
86 fundamental data for establishing and calibrating other models. The eddy covariance method has
87 been widely applied in various ecosystems, including urban areas (Konopka et al., 2021), farmlands
88 (Vote et al., 2015), grasslands (Du et al., 2022a), forests (Kondo et al., 2017), and water bodies (Li
89 et al., 2022).

90 Net Ecosystem Exchange (NEE) of carbon dioxide is a fundamental parameter in the
91 biogeochemical feedback of the climate system (Graf et al., 2013). The carbon flux in forest
92 ecosystems is influenced by multiple environmental factors. Previous studies have shown that NEE
93 is significantly influenced by photosynthetically active radiation (PAR), air temperature (AT), vapor
94 pressure deficit (VPD), relative humidity (RH), and soil temperature (ST) (Liu et al., 2022). Given
95 the projected future global warming trends, the role of forests as a vast carbon reservoir becomes
96 highly significant and worthy of attention. The Qinghai-Tibet Plateau (QTP) is the highest and
97 largest plateau in the world, with an extensive area of alpine forests covering approximately $2.3 \times$
98 10^5 km². These forests hold tremendous economic and ecological benefits. Since the 1960s, the QTP
99 has experienced a faster warming rate compared to lowland areas. It is projected that this
100 phenomenon will be intensified by the end of the 21st century (Li et al., 2019). Currently, the QTP



101 is considered a weak carbon sink at the overall level, but the carbon source-sink dynamics vary
102 among different ecosystems (Chen et al., 2022). For instance, most lakes in the QTP are currently
103 characterized by supersaturated CO₂ levels (Cole et al., 1994). Mu et al.(2023), found that the
104 thermokarst lakes serve as significant carbon sources through carbon flux measurements in 163
105 thermokarst lakes during the summer and autumn seasons. Wang et al.(2021), discovered that these
106 ecosystems act as sinks for carbon dioxide in their study comparing carbon fluxes in ten high-
107 mountain ecosystems with different grassland types. The alpine meadows in the eastern QTP were
108 identified as strong carbon sinks, with the highest annual average NEE recorded at -284 g C m⁻².
109 Forest ecosystems play a crucial role in the south-eastern edge of the QTP, providing important
110 support for climate regulation and forestry-based economic activities. However, the QTP is a vast
111 region, with a widespread distribution of high-altitude and subalpine forests. It is essential for
112 researchers to conduct long-term monitoring to understand how these forests will respond to climate
113 change. Furthermore, there is a significant data gap concerning the monitoring of carbon exchange
114 capacity in the forests of the QTP, indicating the need for further data collection efforts. Based on
115 this, we have established a carbon flux monitoring site in the subalpine ecosystem of the Three
116 Parallel Rivers Region, located on the south-eastern edge of the QTP, it lies in the transitional zone
117 between the Qinghai-Tibet Plateau and the Yunnan-Guizhou Plateau, and is renowned as a global
118 hotspot for biodiversity (Wang et al., 2022). Our research objectives are as follows:

- 119 1) Determine whether the subalpine forests in the Three Parallel Rivers Region act as a carbon
120 sink or source, and quantify the annual uptake or release of carbon dioxide.
- 121 2) Investigate the main environmental factors influencing the carbon exchange process in the
122 subalpine forests and identify the factors with the greatest impact.
- 123 3) Assess the carbon exchange capacity of the subalpine forests in comparison to other
124 ecosystems of the QTP.

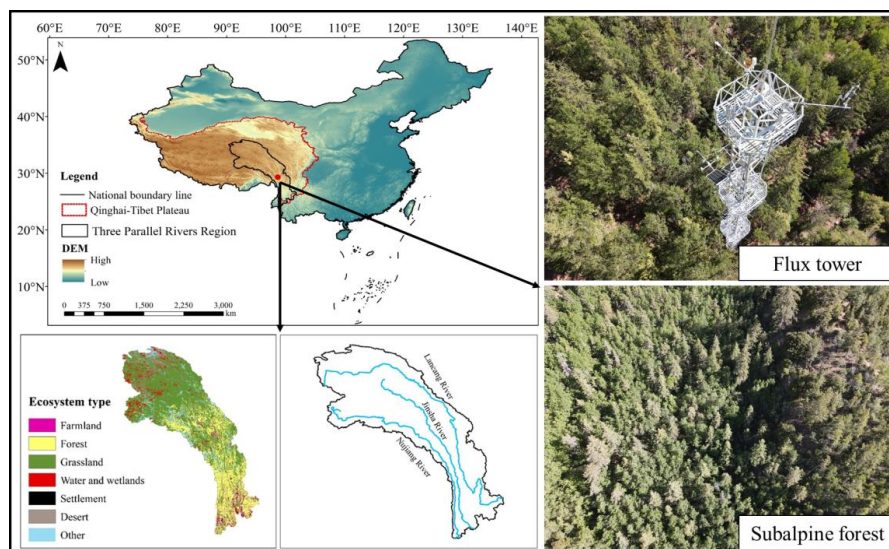
125 This study will provide a data foundation and background support for accurately estimating
126 the carbon balance of forests in high-altitude areas and for model simulations in the future.

127 **2 Materials and Methods**

128 **2.1 Overview of the study site**



129 The study site is located in the Hongla Mountain Yunnan Snub-nosed Monkey National Nature
130 Reserve in Mangkang County, Tibet, China (29.28633 °N, 98.69096 °E). The elevation of the study
131 site is 3755 m. The observation period was from November 2020 to October 2022. The study area
132 experiences large diurnal temperature variations and dry conditions in winter, while the summers
133 are warm and humid. The climate of the region is characterized as a typical mountainous climate.
134 The average daily sunshine duration exceeds 10 h, with an annual average temperature of 5°C and
135 an average annual precipitation of around 600 mm. The main tree species in the area include *Picea*
136 *likiangensis* var. *rubescens*, *Abies squamata*, *Sabina tibetica* Kom, and *Abies ernestii*. They are
137 accompanied by the growth of some *Quercus aquifolioides*, *Rhododendron lapponicum*, and
138 *Potentilla fruticosa* shrubs. The vegetation coverage ranges from 70% to 80%, indicating rich
139 vegetation resources. The dominant soil type is yellow brown soil. The study site is located in the
140 core area of the Three Parallel Rivers (Nujiang River, Lancang River, and Jinsha River) Region.
141 The area exhibits a complex and diverse climatic environment influenced by the southwest and
142 southeast monsoon. The mountainous terrain contributes to distinct vertical climate characteristics
143 and significant variations in water and heat conditions. The region is characterized by numerous dry
144 and hot river valleys and widespread distribution of canyons.



145
146 Figure 1 Overview of the study area (The national boundary range in the figure comes from the
147 <http://bzdt.ch.mnr.gov.cn>, elevation data from www.gscloud.cn.)



148 2.2 Eddy covariance system

149 The flux data in this study were collected from a 35 m-high tower located at the study site. At
150 the top of the tower, a 3-D wind velocity (Wind Master, Gill, UK) and an open-path infrared
151 CO₂/H₂O analyzer (LI-7500DS, Li-Cor, USA) were installed to measure CO₂ flux. The instruments
152 had a response frequency of 10 Hz. Additionally, micro-meteorological sensors were placed at
153 different heights on the tower, including sensors for observing air temperature and humidity
154 (HMP155A, Vaisala, Finland), soil temperature (TEROS11, LI-Cor, USA), and photosynthetically
155 active radiation (LI-190R, LI-Cor, USA), among other environmental variables. All data were
156 recorded at 30-m intervals and stored in a SmartFlux 3 data logger (Li-Cor, USA) for future
157 download.

158 2.3 Data processing and quality control

159 Turbulent transport is the primary form of gas exchange between the near-surface and the
160 atmosphere. In the case of a homogeneous and flat underlying surface, considering only the
161 turbulent transport of substances in the vertical direction, the CO₂ flux F_c ($\mu\text{mol m}^{-2} \text{s}^{-1}$ or mg m^{-2}
162 s^{-1}) within the region can be calculated using the following.

163
$$F_c = \overline{W'CO_2'} \quad (1)$$

164 Where W' represents the vertical component of 3-D wind speed fluctuations (m/s), CO_2' represents
165 the fluctuations in measured CO₂ mole concentration ($\mu\text{mol m}^{-3}$), and the overline denotes the
166 average value over a half-hour time period. A positive value of F_c indicates carbon emissions from
167 the underlying surface during the given time interval, while a negative value represents carbon
168 uptake.

169 The acquired 10 Hz raw data was processed and corrected using the EddyPro software
170 (EddyPro 7.06, Li-Cor, USA). The correction process involved outlier detection for flux data, lag
171 elimination, second-order coordinate rotation (Jia et al., 2020), ultrasonic temperature correction
172 (Schotanus et al., 1983), frequency correction (Moncrieff et al., 1997), and Webb-Pearman-Leuning
173 (WPL) correction (Leuning and King, 1992). We removed outliers caused by environmental
174 disturbances such as power outages, rain, snow, and dust particles that interfered with the instrument.
175 We also corrected errors resulting from non-uniform and non-flat underlying surfaces (Cao et al.,
176 2019). As a result, we obtained half-hourly flux data with associated data quality indicators. To



177 evaluate the turbulence steadiness, we employed the "0-1-2" quality assessment method, which
178 classified flux results into three quality levels: 0 for excellent data quality, 1 for moderate data
179 quality, and 2 for low data quality (Mauder and Foken, 2011). We removed data points labeled with
180 a quality level of "2". We further eliminated flux data with negative values during nighttime since
181 plants do not perform photosynthesis at night. Additionally, we conducted spectral analysis to
182 identify and remove data points with values significantly deviating from normal. Finally, we utilized
183 the friction velocity (U^*) as a criterion and deleted data recorded during nighttime when U^* was
184 less than 0.28 and 0.39 m s^{-1} (Papale et al., 2006).

185 NEE of CO_2 can be represented by the following:

$$186 \quad \text{NEE} = F_C + F_S \quad (2)$$

187 Where NEE represents the net ecosystem exchange of CO_2 , F_C stands for the observed flux during
188 a specific time period, F_S represents the CO_2 storage in the forest canopy, which is assumed to be
189 zero in this case.

190 We used the Michaelis-Menten model to fit the daytime NEE (NEE_{day}) with respect to PAR to
191 fill in the missing values during the daytime (Falge et al., 2001):

$$192 \quad \text{NEE}_{\text{day}} = \frac{a \cdot \text{PAR} \cdot P_{\text{max}}}{a \cdot \text{PAR} + P_{\text{max}}} - R_{\text{day}} \quad (3)$$

193 where: a ($\mu\text{mol CO}_2/\mu\text{mol PAR}$) represents the apparent photosynthetic quantum efficiency, which
194 characterizes the maximum efficiency of converting light energy during photosynthesis. PAR (μmol
195 $\text{m}^{-2} \text{s}^{-1}$) is the photosynthetically active radiation, a measure of the amount of light energy available
196 for photosynthesis. P_{max} ($\mu\text{mol CO}_2 \text{ m}^{-2} \text{ s}^{-1}$) is the apparent maximum photosynthetic rate,
197 representing the maximum CO_2 uptake rate under optimal conditions. R_{day} ($\mu\text{mol CO}_2 \text{ m}^{-2} \text{ s}^{-1}$) is the
198 daytime dark respiration rate, which denotes the rate of CO_2 release during daylight hours. The
199 parameters a , P_{max} , and R_{day} are obtained through non-linear fitting of the Michaelis-Menten model
200 to the observed data.

201 During the nighttime, the NEE is modeled using an exponential function of respiration and soil
202 temperature to fill in the missing values of NEE during the night ($\text{NEE}_{\text{night}}$) (Lloyd and Taylor, 1994;
203 Kato et al., 2006):

$$204 \quad \text{NEE}_{\text{night}} = a \cdot \exp^{(br)} \quad (4)$$



205 The parameters a and b are estimated values for the exponential function used in modeling NEE_{night} .
206 The variable t represents the soil temperature measured at the depth of 5 cm. The data processing
207 software used for this analysis is Origin 2023 (Originlab Corporation, USA). For the missing data,
208 interpolation was performed using Tovi software (Tovi, Li-Cor, USA) that allows for data
209 interpolation to fill in the gaps and ensure a continuous dataset for further analysis (Reichstein et
210 al., 2005).

211 2.4 Flux splitting

212 Ecosystem respiration (RE) is the sum of plant and heterotrophic respiration in an ecosystem
213 and is obtained by adding the measured nighttime data to the extrapolated daytime data. Gross
214 primary productivity (GPP) is the total amount of organic carbon fixed by green plants through
215 photosynthesis per unit of time and per unit of area:

$$216 \quad RE = R_{\text{day}} + R_{\text{night}} \quad (5)$$

$$217 \quad GPP = -NEE + RE \quad (6)$$

218 Carbon use efficiency (CUE) is a crucial parameter that reflects the ability of an ecosystem to
219 sequester carbon. It is defined as the ratio of net primary productivity to gross primary productivity.
220 CUE can be expressed using the following equation:

$$221 \quad CUE = \frac{NEP}{GPP} = \frac{-NEE}{GPP} \quad (7)$$

222 To study the variation of ecosystem respiration rates with environmental conditions, we
223 considered the dependence of nocturnal ecosystem respiration on soil temperature (Pavelka et al.,
224 2007; Mamkin et al., 2023):

$$225 \quad Q_{10} = \exp(10 \cdot \alpha) \quad (8)$$

$$226 \quad \ln(NEE_{\text{night}}) = \alpha \cdot T + \gamma \quad (9)$$

227 Where T is the soil temperature ($^{\circ}\text{C}$) and γ is an empirical parameter of the equation.

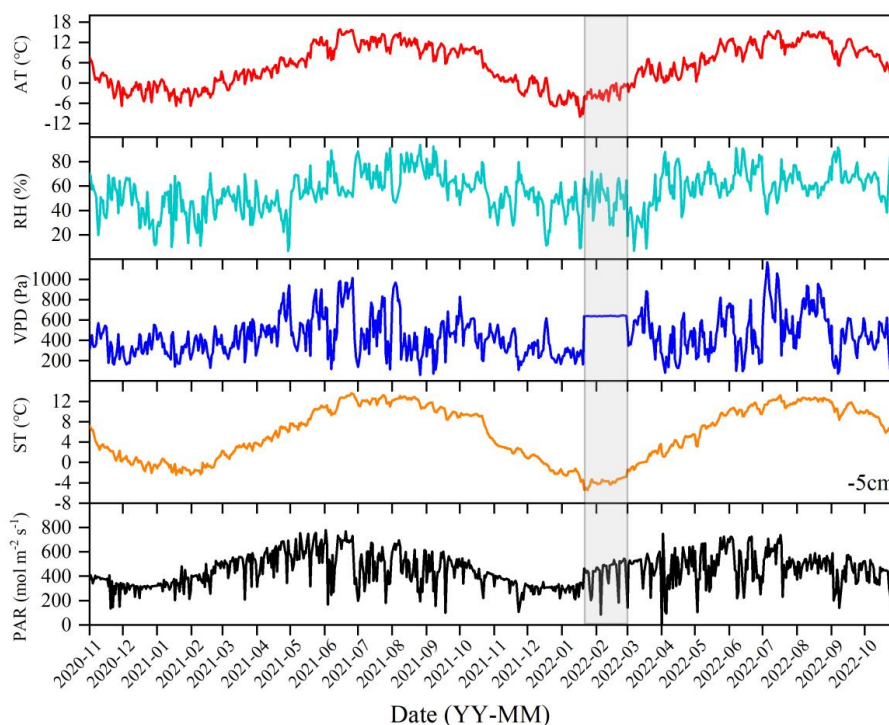
228 3 Results

229 3.1 Daily average changes in main environmental factors

230 During the observational period, the environmental conditions exhibited significant
231 fluctuations. The winter and spring seasons were characterized by cold and dry conditions, while
232 the summer and autumn seasons were warm and humid. The daily maximum air temperature (AT)
233 recorded was 15.87°C (on June 15, 2021), and the minimum temperature was -9.88°C (on January



234 17, 2022), with an average of 5.5 °C over the two-year period. The relative humidity (RH) ranged
235 from a maximum of 93.98% (on August 26, 2021) to a minimum of 6.74% (on April 29, 2021), with
236 an annual average of 55.89%. The vapor pressure deficit (VPD), which represents the difference
237 between the saturated vapor pressure and the actual vapor pressure in the air, influences plant
238 stomatal closure and regulates physiological processes such as transpiration and photosynthesis.
239 The highest recorded VPD was 1169.8 hPa (on July 5, 2022), and the lowest one was 60.8 hPa (on
240 August 26, 2021), with an annual average of 446.4 hPa. Soil temperature (ST) exhibited a similar
241 trend to air temperature and remained relatively stable over short periods. The highest observed soil
242 temperature was 13.53 °C (on June 27, 2021), while the minimum was -3.78 °C (on January 18,
243 2022), with an annual average of 6.11 °C. Photosynthetically active radiation (PAR) reached a
244 maximum value of 779.06 mol m⁻² s⁻¹ (on June 2, 2021), with an annual average of 447.24 mol m⁻²
245 s⁻¹. From March to October, the radiation conditions were favorable for photosynthesis, but
246 reduction in radiation intensity was observed during rainy, snowy, and cloudy weather conditions.



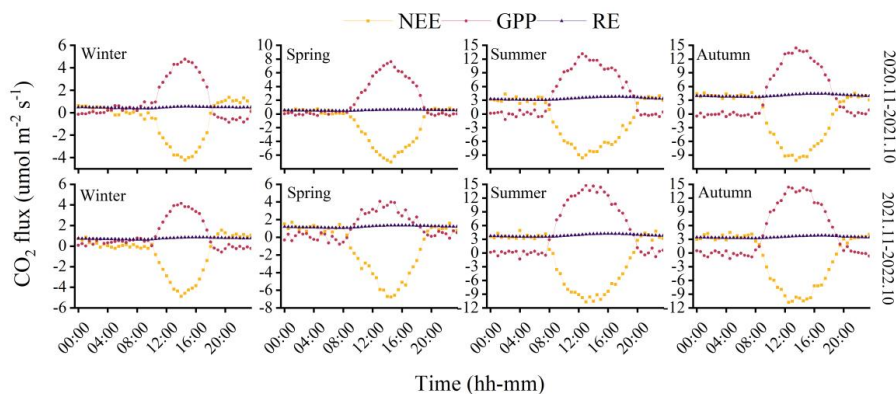
247



248 Figure 2 Characteristics of main environmental factors, air temperature (AT), relative humidity
249 (RH), vapor pressure deficit (VPD), soil temperature (ST), Photosynthetically active radiation
250 (PAR). (The shaded part of the figure represents the data interpolated by the nearby station)

251 3.2 The seasonal variations in NEE, RE, and GPP

252 The observations from the forest ecosystem indicates distinct diurnal and seasonal variations
253 in NEE and GPP. The NEE and GPP exhibit a pronounced U-shaped curve, with significant seasonal
254 differences. The summer and autumn are characterized by peak carbon uptake, with the maximum
255 NEE reaching $10.78 \text{ umol CO}_2 \text{ m}^{-2} \text{ s}^{-1}$ (12:30, autumn). During the nighttime, the ecosystem
256 generally releases carbon, while during favorable daytime meteorological conditions, it
257 demonstrates carbon uptake. The peak carbon absorption of the forest ecosystem occurs from 12:00
258 to 15:00 (Beijing time, UTC+8:00). The carbon sequestration period in summer and autumn is 1.5-
259 3 hrs longer than in winter. The timing of maximum carbon sequestration capacity changes with
260 each season. In winter, the transition from nighttime carbon release to daytime carbon uptake occurs
261 around 08:30, while in summer, it shifts to around 07:30 (Beijing time, UTC+8:00). GPP reflects
262 the carbon sequestration capacity of the forest, with the recorded daily total productivity highest at
263 $14.76 \text{ umol CO}_2 \text{ m}^{-2} \text{ s}^{-1}$ during summer season of second year, RE exhibits minor diurnal variations
264 but shows significant seasonal differences, with maximum and minimum diurnal RE values of 0.73
265 $\text{umol CO}_2 \text{ m}^{-2} \text{ s}^{-1}$ and $0.17 \text{ umol CO}_2 \text{ m}^{-2} \text{ s}^{-1}$, respectively. The respiration rate of the coniferous
266 forest during the summer and autumn is 5-8 times higher than that in the winter and spring.



267

268

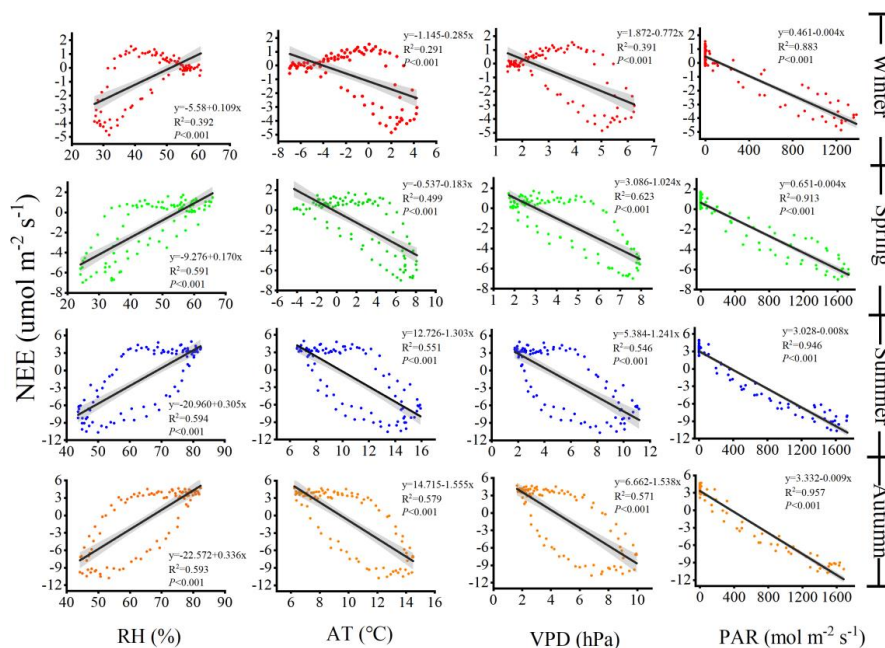
Figure 3 The monthly variations in carbon fluxes

269

3.3 Relationship between NEE and main environmental factors



270 The fitting results between NEE and environmental factors indicate that the selected
 271 environmental factors have a significant impact on NEE ($P < 0.001$) (Figure 4). However, the
 272 influence of individual environmental factors on NEE varies across different seasons. RH has the
 273 smallest impact on NEE during the summer, while AT, VPD, and PAR exhibit the strongest
 274 influence on NEE during the autumn. These factors consistently have the least impact on NEE
 275 during autumn. In the same season, PAR primarily controls NEE, with an R^2 value reaching up to
 276 0.957. Positive values of NEE indicate carbon emissions, while negative values indicate carbon
 277 uptake. Therefore, air temperature, vapor pressure deficit, and PAR all have a significant positive
 278 effect on carbon uptake, while an increase in humidity leads to a noticeable reduction in carbon
 279 uptake.



280

281

Figure 4 Relationship between NEE and main environmental factors

282

3.4 Seasonal variation characteristics of NEE, GPP, and RE

283

284

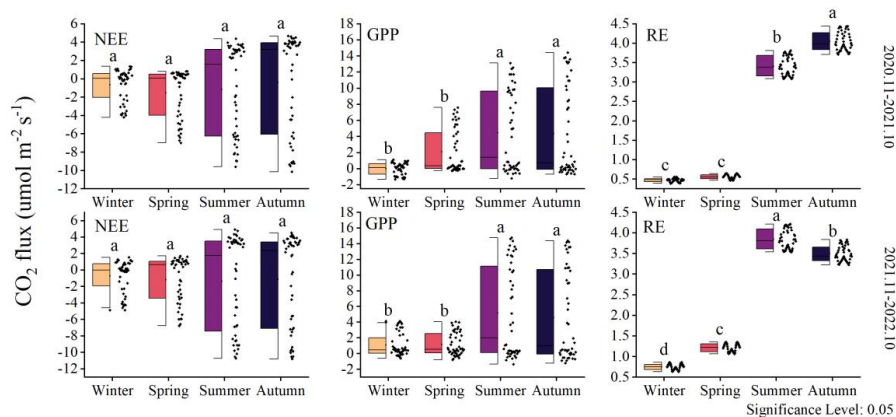
285

286

The NEE rate did not show significant inter-seasonal differences (Figure 5). However, data distribution indicates that the variability in NEE rate differs across different seasons, particularly between the growing seasons (summer, autumn) and the non-growing seasons (winter, spring). The changes in GPP over the two years were similar, with significant differences observed between the



287 growing seasons and the non-growing seasons ($P < 0.05$). The RE was higher during the growing
 288 seasons compared to the non-growing seasons. The forest ecosystem respiration rate was lowest in
 289 winter and slightly higher in spring. The highest ecosystem respiration occurred in the first year
 290 during autumn, while in the second year, it was highest during summer. This pattern is also reflected
 291 in GPP and NEE.



292

293

Figure 5 Seasonal variation of carbon fluxes

294

3.5 Changes in total NEE, GPP, RE, and CUE

295

296

297

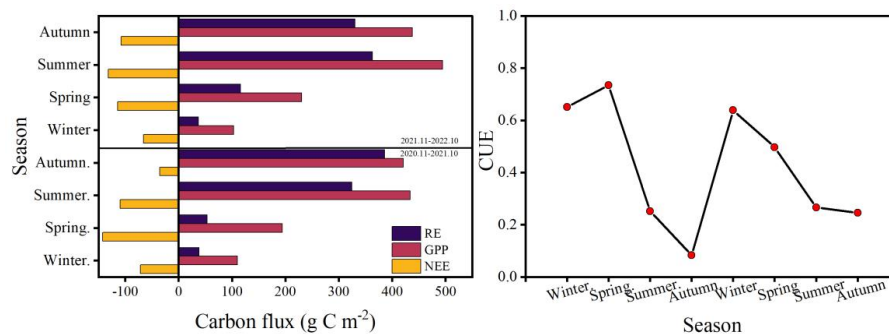
298

299

300

301

The cumulative fluxes over the two years for the forest ecosystem are shown in Figure 6. NEE indicates the net carbon sequestration in each month. The cumulative respiration reached its highest value of 363.23 g C m⁻² in the summer of 2022. The total NEE, GPP, and RE for the first year were -358.65, 1159.60, and 802.67 g C m⁻², respectively, and -419.41, 1265.96, and 846.55 g C m⁻² for the second year, respectively. The CUE was higher during the cold non-growing seasons and lower during the growing seasons, with a maximum value of 0.73 and a minimum value of 0.08. The average CUE over the two years was 0.43 and 0.41, respectively.



302

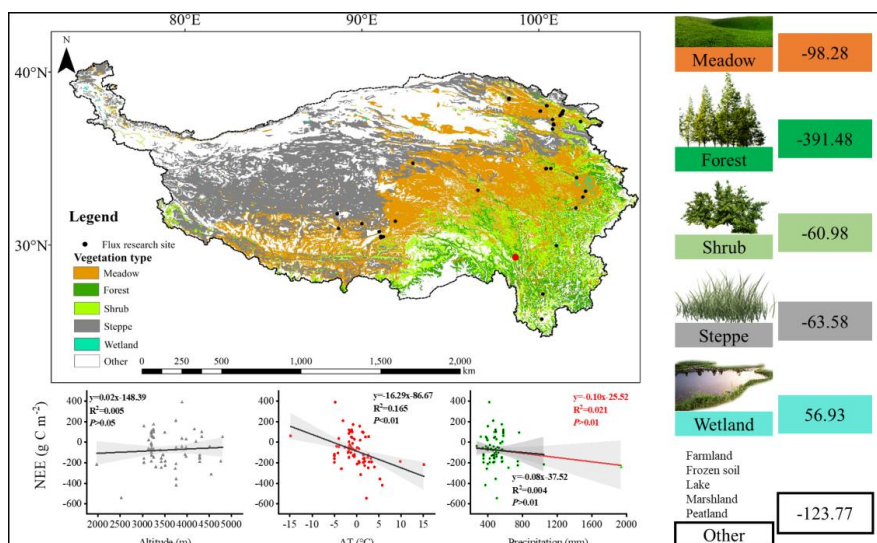


303 Figure 6 Change in total carbon flux and carbon use efficiency

304 3.6 The carbon sequestration potential of subalpine forests of QTP

305 To clarify the carbon sequestration contribution of the subalpine forests found on the QTP, we
 306 collected and compared 83 research results from 49 studies that utilized EC systems (Figure 7).
 307 Ecosystems with high vegetation cover exhibited higher annual cumulative carbon sequestration.
 308 Among these ecosystems, the subalpine forests on the QTP showed the highest carbon sequestration
 309 potential, reaching an average of 391.48 g C m⁻² per year. The carbon sequestration potential of
 310 different ecosystems ranked as follows: forest > meadow > steppe > shrub. The average value for
 311 wetlands indicated that they are a significant source of CO₂, releasing 56.93 g C m⁻² into the
 312 atmosphere annually.

313 We also analyzed the influence of elevation, mean annual temperature, and precipitation on
 314 NEE at these sites in the QTP. It was found that increasing elevation had a negative impact on
 315 carbon uptake, while higher mean annual temperatures significantly increased carbon uptake. Mean
 316 annual precipitation had a weak influence on NEE. These findings highlight the important role of
 317 subalpine forests in carbon sequestration in the QTP and provide insights into the factors that affect
 318 carbon exchange on the QTP, such as altitude, temperature, and precipitation.



319

320 Figure 7 Carbon exchange potential of different ecosystems in the Qinghai-Tibet Plateau

321 **4 Discussion**



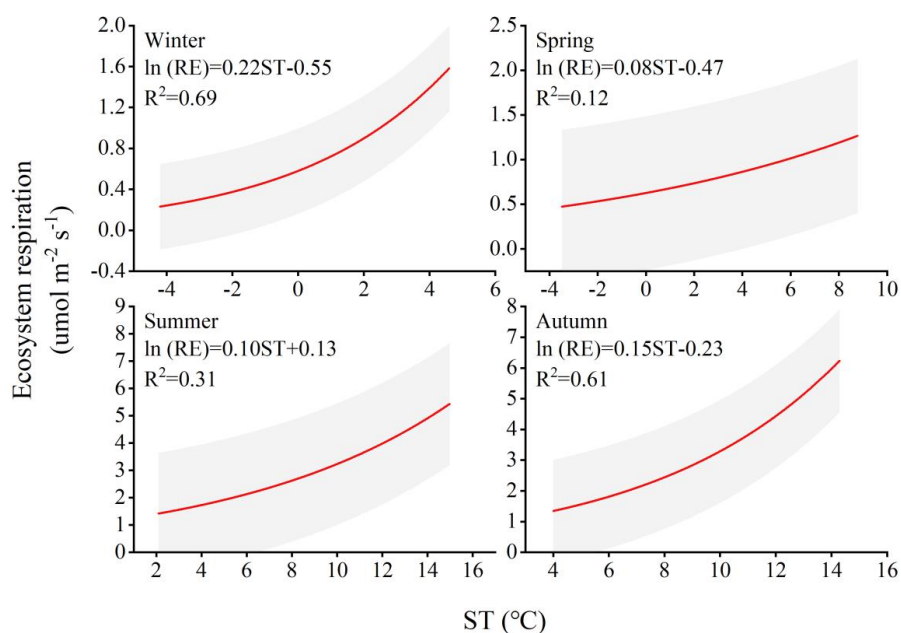
322 4.1 Main factors affecting the carbon sequestration function of subalpine forests

323 Climate change is the significant factor affecting the vegetation's carbon sequestration capacity,
324 particularly at the seasonal scale due to phenological changes (Acosta-Hernández et al., 2020). Our
325 study has demonstrated that, in the short term, NEE is primarily influenced by factors such as PAR,
326 AT, RH, and VPD. These factors play a role in regulating vegetation photosynthesis and,
327 consequently, carbon uptake. For instance, PAR represents the portion of solar energy that can be
328 utilized by plants and is an essential component in chloroplast reactions. AT regulates the activity
329 of enzymes involved in light and dark reactions, which may contribute to seasonal variations in
330 NEE. RH and VPD impact the entire process of photosynthesis by influencing the concentration of
331 CO₂ in the air and the stomatal conductance (the pathway for CO₂ exchange). In different seasons,
332 the same influencing factors exhibit varying degrees of contribution to NEE. For example, during
333 winter, when the climatic conditions are relatively harsh with low air temperature and humidity, the
334 forest maintains a low level of carbon uptake. While the forest continues to absorb carbon dioxide,
335 the uptake remains limited at a low level under such unfavorable conditions. On longer time scales,
336 such as annual and decadal variations, the inherent changes in forest NEE may be attributed to
337 disturbances and recovery (Hayek et al., 2018). Research by Amiro (2001) has demonstrated that
338 disturbances caused by fire and logging have been found to regulate the carbon balance of northern
339 forests in Canada over several decades. Additionally, there are close relationships between subtle
340 climate changes, stand dynamics, tree age, post-disturbance time, and forest carbon storage and
341 cycling (Bradford et al., 2008). Compared to naturally regenerating forests, actively restored forests
342 exhibit higher rates of carbon accumulation. Restoration efforts have been shown to increase
343 aboveground carbon density recovery rates by more than 50% over a decade, from 2.9 to 4.4
344 megagrams per hectare per year (Philipson et al., 2020). The carbon dioxide generated by soil
345 microbial activity is an essential component of forest ecosystem respiration. Soils contain the largest
346 organic carbon reservoir on Earth, three times more than the carbon content in the atmosphere (Tifafi
347 et al., 2018). With climate warming, soil microorganisms, and root systems will decompose soil
348 organic carbon at a faster rate, releasing carbon dioxide into the atmosphere more rapidly.
349 Temperature plays a more sensitive role in soil carbon turnover in cold climate regions compared
350 to warmer conditions (Koven et al., 2017). Ecological respiration sensitivity to temperature is



351 represented by the Q_{10} coefficient. In this study, seasonal variations influenced the magnitude of
352 Q_{10} (as shown in Figure 8). The calculated Q_{10} values for each season are as follows: 9.025, 2.22,
353 2.71, and 4.48. The winter season exhibited the highest sensitivity of forest ecosystem respiration
354 to temperature, indicating that respiration rates in the winter are more responsive to changes in
355 temperature compared to other seasons.

356 Our integrated analysis (as shown in Figure 7) reveals that, despite the high elevation of the
357 "Third Pole", the topographic factor of elevation does not have a significant impact on carbon uptake.
358 Instead, NEE gradually increases with a steep rise in elevation. Research conducted by WANG et
359 al.(2023b), indicates that average temperature and precipitation are the main driving factors of
360 interannual variations in NEE in alpine meadows and alpine grasslands. Decreased precipitation can
361 cause some regions of high precipitation-dependent alpine grasslands to transition into carbon
362 sources. It is worth noting that, among all data collection sites, alpine wetlands show an average
363 carbon source trend. Due to prolonged flooding and low temperatures, microbial activity in alpine
364 wetlands is hindered, and the accumulation of organic carbon from plant litter decomposition is
365 substantial. As a result, approximately 56.93 g C m^{-2} is emitted into the atmosphere annually.
366 Previous studies have indicated that NEE in alpine wetlands is increasing with global warming
367 (Yasin et al., 2022).





369 Figure 8 Relationship between NEE_{night} and 5 cm depth soil temperature in different seasons

370 4.2 Sustained carbon sequestration of subalpine forests

371 Subalpine forests are integral components of global alpine ecosystems and play crucial roles
372 in the global carbon cycle. It is worth noting that atmospheric carbon dioxide levels are steadily
373 increasing due to human activities. Mitigation of greenhouse gas emissions to achieve carbon
374 neutrality through natural processes is undoubtedly the most cost-effective and convenient option,
375 in addition to industrial carbon reduction measures. Therefore, understanding whether natural
376 ecosystems possess sustained carbon sequestration functionality is of utmost importance. Tian.
377 (2018), used a structural-dynamic approach to predict that US forests will continue to sequester
378 carbon for majority of the next century, sequestering 128 Tg C year⁻¹. Consistent with our findings,
379 our study on subalpine forests demonstrates that they continue to absorb carbon dioxide even during
380 winter, which aligns well with measurements taken in the vicinity of Mount Fuji in Japan
381 (Mizoguchi et al., 2012). Furthermore, their research further confirms that northern forests exhibit
382 higher carbon uptake capacity. The age of subalpine forests is a crucial factor influencing sustained
383 carbon sequestration. Based on NPP simulations of natural subalpine forests in the Northern Rockies,
384 Carey. (2001), found that aboveground net primary productivity reaches its maximum after
385 approximately 250 years, followed by a decline. This challenges previous notions regarding the
386 carbon sequestration potential of forests that are approximately over 100 years of age. In our study,
387 the subalpine forest exhibited a sparse shrub understory, indicating that it is not a mature forest
388 ecosystem. This may be a significant factor contributing to its stronger carbon sequestration capacity
389 compared to the high-mountain forests (mature forests) in Mount Gongga in the QTP (Yuanyuan et al.,
390 et al., 2018). However, its carbon sequestration ability is slightly weaker than that of the Qilian
391 Mountains high-mountain forests (approximately 60-70 years old) in the QTP (Yuanyuan et al.,
392 2018; Du et al., 2022b). Although existing flux monitoring results of high-altitude forests in the
393 QTP indicate that these forest ecosystems act as carbon sinks, it is important to consider that globally
394 there are still many cold regions where coniferous forests serve as carbon sources. For example,
395 continuous CO₂ flux monitoring from native boreal forests in Sweden for over 10 years indicates
396 that they are a net carbon source, this is attributed to the contribution of woody debris to RE due to
397 disturbances such as extreme weather events, fires, insect infestations, and pathogen attacks



398 (Hadden and Grelle, 2017). In the summer of 2018, Europe experienced a heatwave that affected
399 the carbon cycling in forests. The southern Estonian mixed coniferous-deciduous forest, under the
400 influence of the heatwave, transitioned from a net carbon sink to a net carbon source in 2018
401 (Krasnova et al., 2022). Particular attention should be paid to the long-term monitoring in high-
402 altitude environments of the impact of disturbances on forest carbon sequestration capacity. Our
403 study has shown that forests in the QTP have the strongest carbon sink capacity, indicating that
404 alpine forests will have an important sustained effect on carbon reduction in the QTP in the context
405 of future climate change, but whether this sustained effect will be longer than other ecosystems is
406 still unknown. However, a modeling experiment in a large semi-arid area of California predicted
407 that grasslands are more resilient carbon sinks than forests in responding to climate change in the
408 21st century (Dass et al., 2018). In terms of carbon sequestration rate, forests on the QTP were
409 significantly stronger than other ecosystems, followed by grasslands, while alpine deserts and alpine
410 grasslands in the north-western and southern regions were the main carbon sources (Wu et al., 2022).
411 Forests are mostly distributed in the south-eastern margin of the QTP and the mid-altitude area near
412 3000 m in the Sichuan-Tibet alpine gorge area, with an area of $19.3 \times 10^4 \text{ km}^2$ (Y et al., 2022).
413 Based on the average value of a few current carbon flux monitoring, the forest in the QTP will
414 absorb about $75.5 \times 10^5 \text{ T C year}^{-1}$.

415 **5 Conclusion**

416 This study explores the carbon sequestration function, seasonal variations, and climate drivers
417 of subalpine forests in the QTP. Over the observational period, environmental factors exhibited
418 significant fluctuations, with cold and dry conditions prevailing during winter and spring, while
419 warm and moist conditions characterized the summer and autumn seasons. The research reveals that
420 the subalpine forest possesses enormous carbon sequestration potential, with a total NEE, GPP, and
421 RE of -358.65, 1159.60, and 802.67 g C m^{-2} , respectively, and -419.41, 1265.96, and 846.55 g C m^{-2}
422 for two years, respectively. Individual environmental factors exhibited varying effects on NEE in
423 different seasons, with relative humidity having the least impact on NEE during summer, while air
424 temperature, saturated vapor pressure deficit, and photosynthetically active radiation had the most
425 significant influence during autumn, with minimal effects from these factors during other seasons.
426 Moreover, photosynthetically active radiation was identified as the primary control of NEE in the



427 same season. The NEE rate did not exhibit significant differences across seasons. Combining results
428 from other eddy covariance sites on the QTP, this study highlights those forests have the highest
429 carbon sequestration potential, reaching 391.48g C m⁻² annually, followed by meadows, steppes,
430 and shrubs. Wetlands, however, were identified as substantial carbon dioxide source. Despite the
431 challenges posed by climate change, the subalpine forests in the QTP retain substantial carbon
432 sequestration potential. Strengthening conservation and management efforts for subalpine forests is
433 crucial to ensure their continued and significant carbon sequestration function in the future. Overall,
434 this research underscores the vital role of subalpine forests in the QTP as essential carbon sink
435 regions, playing a critical role in the context of global climate change.

436 **Data availability.** The data are available from the authors on request.

437 **Authorship contributions.** **Niu Zhu:** Conceptualization, study design, data analyses,
438 visualization, writing-original draft. **JinNiu Wang:** study design, writing—review & editing,
439 supervision, project administration, funding acquisition. **Dongliang Luo and Xufeng Wang:**
440 writing-reviewing & editing. **Cheng Shen and Ning Wu:** resources, data curation, supervision. all
441 authors approved the final manuscript.

442 **Declaration of competing interest.** The authors declare that they have no conflict of interest.

443 **Acknowledgements.** We thank Ms. Neha Bisht for her substantial comments and language
444 revision on improving the manuscript. This study was funded by CAS "Light of West China"
445 Program (2021XBZG-XBQNXZ-A-007); National Natural Science Foundation of China
446 (31971436); State Key Laboratory of Cryospheric Science, Northwest Institute of Eco-Environment
447 and Resources, Chinese Academy Sciences (SKLCS-OP-2021-06).

448 **Reference**

449 Acosta-Hernández, A. C., Padilla-Martínez, J. R., Hernández-Díaz, J. C., Prieto-Ruiz, J. A., Goche-Telles,
450 J. R., Nájera-Luna, J. A., and Pompa-García, M.: Influence of Climate on Carbon Sequestration in
451 Conifers Growing under Contrasting Hydro-Climatic Conditions, *Forests*, 11, 1134, 2020.
452 Amiro, B. D.: Paired-tower measurements of carbon and energy fluxes following disturbance in the
453 boreal forest, *Global Change Biology*, 7, 253-268, 10.1046/j.1365-2486.2001.00398.x, 2001.



- 454 Anderson, D. E., Verma, S. B., and Rosenberg, N. J.: Eddy correlation measurements of CO₂, latent
455 heat, and sensible heat fluxes over a crop surface, *Boundary-Layer Meteorology*, 29, 263-272, 1984.
- 456 Bradford, J. B., Birdsey, R. A., Joyce, L. A., and Ryan, M. G.: Tree age, disturbance history, and carbon
457 stocks and fluxes in subalpine Rocky Mountain forests, *Global Change Biology*, 14, 2882-2897,
458 10.1111/j.1365-2486.2008.01686.x, 2008.
- 459 Cai, W., He, N., Li, M., Xu, L., Wang, L., Zhu, J., Zeng, N., Yan, P., Si, G., and Zhang, X.: Carbon
460 sequestration of Chinese forests from 2010 to 2060: Spatiotemporal dynamics and its regulatory
461 strategies, *Science Bulletin*, 67, 836-843, 2022.
- 462 Cao, S., Cao, G., Chen, K., Han, G., Liu, Y., Yang, Y., and Li, X.: Characteristics of CO₂, water vapor,
463 and energy exchanges at a headwater wetland ecosystem of the Qinghai Lake, *Canadian Journal of Soil
464 Science*, 99, 227-243, 10.1139/cjss-2018-0104, 2019.
- 465 Carey, E. V., Sala, A., Keane, R., and Callaway, R. M.: Are old forests underestimated as global carbon
466 sinks?, *Global Change Biology*, 7, 339-344, 10.1046/j.1365-2486.2001.00418.x, 2001.
- 467 Chen, H., Ju, P. J., Zhu, Q., Xu, X. L., Wu, N., Gao, Y. H., Feng, X. J., Tian, J. Q., Niu, S. L., Zhang, Y.
468 J., Peng, C. H., and Wang, Y. F.: Carbon and nitrogen cycling on the Qinghai-Tibetan Plateau, *NATURE
469 REVIEWS EARTH & ENVIRONMENT*, 3, 701-716, 10.1038/s43017-022-00344-2, 2022.
- 470 Cole, J. J., Caraco, N. F., Kling, G. W., and Kratz, T. K.: Carbon dioxide supersaturation in the surface
471 waters of lakes, *Science*, 265, 1568-1570, 1994.
- 472 Dass, P., Houlton, B. Z., Wang, Y., and Warlind, D.: Grasslands may be more reliable carbon sinks than
473 forests in California, *Environmental Research Letters*, 13, 074027, 10.1088/1748-9326/aacb39, 2018.
- 474 Du, C., Zhou, G., and Gao, Y.: Grazing exclusion alters carbon flux of alpine meadow in the Tibetan
475 Plateau, *Agricultural and Forest Meteorology*, 314, 108774, 2022a.
- 476 Du, Y., Pei, W., Zhou, H., Li, J., Wang, Y., and Chen, K.: Net ecosystem exchange of carbon dioxide
477 fluxes and its driving mechanism in the forests on the Tibetan Plateau, *Biochemical Systematics and
478 Ecology*, 103, 10.1016/j.bse.2022.104451, 2022b.
- 479 Ebermayer, E.: Die gesammte Lehre der Waldstreu mit Rücksicht auf die chemische Statik des
480 Waldbaues: unter Zugrundlegung der in den Königl. Staatsforsten Bayerns angestellten Untersuchungen,
481 Springer1876.
- 482 Falge, E., Baldocchi, D., Olson, R., Anthoni, P., Aubinet, M., Bernhofer, C., Burba, G., Ceulemans, R.,



483 Clement, R., Dolman, H., Granier, A., Gross, P., Grünwald, T., Hollinger, D., Jensen, N.-O., Katul, G.,
484 Keronen, P., Kowalski, A., Lai, C. T., Law, B. E., Meyers, T., Moncrieff, J., Moors, E., Munger, J. W.,
485 Pilegaard, K., Rannik, Ü., Rebmann, C., Suyker, A., Tenhunen, J., Tu, K., Verma, S., Vesala, T., Wilson,
486 K., and Wofsy, S.: Gap filling strategies for defensible annual sums of net ecosystem exchange,
487 *Agricultural and Forest Meteorology*, 107, 43-69, [https://doi.org/10.1016/S0168-1923\(00\)00225-2](https://doi.org/10.1016/S0168-1923(00)00225-2), 2001.
488 Fortunato, A., Herwartz, H., López, R. E., and Figueroa B, E.: Carbon dioxide atmospheric concentration
489 and hydrometeorological disasters, *Natural Hazards*, 112, 57-74, 2022.
490 Graf, A., Werner, J., Langensiepen, M., van de Boer, A., Schmidt, M., Kupisch, M., and Vereecken, H.:
491 Validation of a minimum microclimate disturbance chamber for net ecosystem flux measurements,
492 *Agricultural and forest meteorology*, 174, 1-14, 2013.
493 Hadden, D. and Grelle, A.: Net CO₂ emissions from a primary boreo-nemoral forest over a 10year period,
494 *Forest Ecology and Management*, 398, 164-173, <https://doi.org/10.1016/j.foreco.2017.05.008>, 2017.
495 Hayek, M. N., Longo, M., Wu, J., Smith, M. N., Restrepo-Coupe, N., Tapajos, R., da Silva, R., Fitzjarrald,
496 D. R., Camargo, P. B., Hutyrá, L. R., Alves, L. F., Daube, B., Munger, J. W., Wiedemann, K. T., Saleska,
497 S. R., and Wofsy, S. C.: Carbon exchange in an Amazon forest: from hours to years, *Biogeosciences*, 15,
498 4833-4848, [10.5194/bg-15-4833-2018](https://doi.org/10.5194/bg-15-4833-2018), 2018.
499 Jia, X., Mu, Y., Zha, T., Wang, B., Qin, S., and Tian, Y.: Seasonal and interannual variations in ecosystem
500 respiration in relation to temperature, moisture, and productivity in a temperate semi-arid shrubland,
501 *Science of The Total Environment*, 709, 136210, <https://doi.org/10.1016/j.scitotenv.2019.136210>, 2020.
502 KATO, T., TANG, Y., GU, S., HIROTA, M., DU, M., LI, Y., and ZHAO, X.: Temperature and biomass
503 influences on interannual changes in CO₂ exchange in an alpine meadow on the Qinghai-Tibetan Plateau,
504 *Global Change Biology*, 12, 1285-1298, <https://doi.org/10.1111/j.1365-2486.2006.01153.x>, 2006.
505 Kondo, M., Saitoh, T. M., Sato, H., and Ichii, K.: Comprehensive synthesis of spatial variability in carbon
506 flux across monsoon Asian forests, *Agricultural and Forest Meteorology*, 232, 623-634, 2017.
507 Konopka, J., Heusinger, J., and Weber, S.: Extensive Urban Green Roof Shows Consistent Annual Net
508 Uptake of Carbon as Documented by 5 Years of Eddy-Covariance Flux Measurements, *Journal of*
509 *Geophysical Research: Biogeosciences*, 126, e2020JG005879, 2021.
510 Koven, C. D., Hugelius, G., Lawrence, D. M., and Wieder, W. R.: Higher climatological temperature
511 sensitivity of soil carbon in cold than warm climates, *Nature Climate Change*, 7, 817+,



- 512 10.1038/nclimate3421, 2017.
- 513 Krasnova, A., Mander, Ů., Noe, S. M., Uri, V., Krasnov, D., and Soosaar, K.: Hemiboreal forests' CO₂
514 fluxes response to the European 2018 heatwave, *Agricultural and Forest Meteorology*, 323, 109042,
515 <https://doi.org/10.1016/j.agrformet.2022.109042>, 2022.
- 516 Landsberg, J. and Waring, R.: A generalised model of forest productivity using simplified concepts of
517 radiation-use efficiency, carbon balance and partitioning, *Forest ecology and management*, 95, 209-228,
518 1997.
- 519 Laurin, G. V., Chen, Q., Lindsell, J. A., Coomes, D. A., Del Frate, F., Guerriero, L., Pirotti, F., and
520 Valentini, R.: Above ground biomass estimation in an African tropical forest with lidar and hyperspectral
521 data, *ISPRS Journal of Photogrammetry and Remote Sensing*, 89, 49-58, 2014.
- 522 Le Quéré, C., Andrew, R. M., Friedlingstein, P., Sitch, S., Pongratz, J., Manning, A. C., Korsbakken, J.
523 I., Peters, G. P., Canadell, J. G., and Jackson, R. B.: Global carbon budget 2017, *Earth System Science
524 Data*, 10, 405-448, 2018.
- 525 Leuning, R. and King, K. M.: Comparison of eddy-covariance measurements of CO₂ fluxes by open-
526 and closed-path CO₂ analysers, *Boundary-Layer Meteorology*, 59, 297-311, 10.1007/BF00119818, 1992.
- 527 Li, L., Zhang, Y., Wu, J., Li, S., Zhang, B., Zu, J., Zhang, H., Ding, M., and Paudel, B.: Increasing
528 sensitivity of alpine grasslands to climate variability along an elevational gradient on the Qinghai-Tibet
529 Plateau, *Science of the Total Environment*, 678, 21-29, 2019.
- 530 Li, X. Y., Shi, F. Z., Ma, Y. J., Zhao, S. J., and Wei, J. Q.: Significant winter CO₂ uptake by saline lakes
531 on the Qinghai-Tibet Plateau, *Global Change Biology*, 28, 2041-2052, 2022.
- 532 Liu, C., Wu, Z., Hu, Z., Yin, N., Islam, A. T., and Wei, Z.: Characteristics and influencing factors of
533 carbon fluxes in winter wheat fields under elevated CO₂ concentration, *Environmental Pollution*, 307,
534 119480, 2022.
- 535 Lloyd, J. and Taylor, J. A.: On the temperature dependence of soil respiration, *Functional Ecology*, 8,
536 315-323, 1994.
- 537 Mamkin, V., Avilov, V., Ivanov, D., Varlagin, A., and Kurbatova, J.: Interannual variability in the
538 ecosystem CO₂ fluxes at a paludified spruce forest and ombrotrophic bog in the southern taiga,
539 *Atmospheric Chemistry and Physics*, 23, 2273-2291, 10.5194/acp-23-2273-2023, 2023.
- 540 Mauder, M. and Foken, T.: Documentation and Instruction Manual of the Eddy-Covariance Software



541 Package TK3 (update),
542 Mercer, J. H.: West Antarctic ice sheet and CO₂ greenhouse effect: a threat of disaster, *Nature*, 271, 321-
543 325, 1978.
544 Mizoguchi, Y., Ohtani, Y., Takanashi, S., Iwata, H., Yasuda, Y., and Nakai, Y.: Seasonal and interannual
545 variation in net ecosystem production of an evergreen needleleaf forest in Japan, *Journal of Forest*
546 *Research*, 17, 283-295, 10.1007/s10310-011-0307-0, 2012.
547 Moncrieff, J. B., Massheder, J. M., de Bruin, H., Elbers, J., Friborg, T., Heusinkveld, B., Kabat, P., Scott,
548 S., Soegaard, H., and Verhoef, A.: A system to measure surface fluxes of momentum, sensible heat, water
549 vapour and carbon dioxide, *Journal of Hydrology*, 188-189, 589-611, <https://doi.org/10.1016/S0022->
550 [1694\(96\)03194-0](https://doi.org/10.1016/S0022-1694(96)03194-0), 1997.
551 Mu, C., Mu, M., Wu, X., Jia, L., Fan, C., Peng, X., Ping, C. I., Wu, Q., Xiao, C., and Liu, J.: High carbon
552 emissions from thermokarst lakes and their determinants in the Tibet Plateau, *Global Change Biology*,
553 2023.
554 Pan, Y., Birdsey, R. A., Fang, J., Houghton, R., Kauppi, P. E., Kurz, W. A., Phillips, O. L., Shvidenko, A.,
555 Lewis, S. L., and Canadell, J. G.: A large and persistent carbon sink in the world's forests, *Science*, 333,
556 988-993, 2011.
557 Papale, D., Reichstein, M., Aubinet, M., Canfora, E., Bernhofer, C., Kutsch, W., Longdoz, B., Rambal,
558 S., Valentini, R., Vesala, T., and Yakir, D.: Towards a standardized processing of Net Ecosystem
559 Exchange measured with eddy covariance technique: algorithms and uncertainty estimation,
560 *Biogeosciences*, 3, 571-583, 10.5194/bg-3-571-2006, 2006.
561 Pavelka, M., Acosta, M., Marek, M. V., Kutsch, W., and Janous, D.: Dependence of the Q₁₀ values on
562 the depth of the soil temperature measuring point, *Plant and Soil*, 292, 171-179, 10.1007/s11104-007-
563 9213-9, 2007.
564 Philipson, C. D., Cutler, M. E. J., Brodrick, P. G., Asner, G. P., Boyd, D. S., Costa, P. M., Fiddes, J.,
565 Foody, G. M., van der Heijden, G. M. F., Ledo, A., Lincoln, P. R., Margrove, J. A., Martin, R. E., Milne,
566 S., Pinard, M. A., Reynolds, G., Snoep, M., Tangki, H., Wai, Y. S., Wheeler, C. E., and Burslem, D. F. R.
567 P.: Active restoration accelerates the carbon recovery of human-modified tropical forests, *Science*, 369,
568 838-+, 10.1126/science.aay4490, 2020.
569 Reichstein, M., Falge, E., Baldocchi, D., Papale, D., Aubinet, M., Berbigier, P., Bernhofer, C., Buchmann,



570 N., Gilmanov, T., Granier, A., Grünwald, T., Havránková, K., Ilvesniemi, H., Janous, D., Knohl, A.,
571 Laurila, T., Lohila, A., Loustau, D., Matteucci, G., Meyers, T., Miglietta, F., Ourcival, J.-M., Pumpanen,
572 J., Rambal, S., Rotenberg, E., Sanz, M., Tenhunen, J., Seufert, G., Vaccari, F., Vesala, T., Yakir, D., and
573 Valentini, R.: On the separation of net ecosystem exchange into assimilation and ecosystem respiration:
574 review and improved algorithm, *Global Change Biology*, 11, 1424-1439, <https://doi.org/10.1111/j.1365->
575 2486.2005.001002.x, 2005.

576 Schotanus, P., Nieuwstadt, F. T. M., and De Bruin, H. A. R.: Temperature measurement with a sonic
577 anemometer and its application to heat and moisture fluxes, *Boundary-Layer Meteorology*, 26, 81-93,
578 10.1007/BF00164332, 1983.

579 Stein, T.: Carbon dioxide peaks near 420 parts per million at Mauna Loa observatory, NOAA Research,
580 June, 7, 2021.

581 Swinbank, W.: The measurement of vertical transfer of heat and water vapor by eddies in the lower
582 atmosphere, *Journal of Atmospheric Sciences*, 8, 135-145, 1951.

583 Tian, X., Sohngen, B., Baker, J., Ohrel, S., and Fawcett, A. A.: Will US forests continue to be a carbon
584 sink?, *Land Economics*, 94, 97-113, 2018.

585 Tifafi, M., Guenet, B., and Hatte, C.: Large Differences in Global and Regional Total Soil Carbon Stock
586 Estimates Based on SoilGrids, HWSD, and NCSCD: Intercomparison and Evaluation Based on Field
587 Data From USA, England, Wales, and France, *Global Biogeochemical Cycles*, 32, 42-56,
588 10.1002/2017gb005678, 2018.

589 Vote, C., Hall, A., and Charlton, P.: Carbon dioxide, water and energy fluxes of irrigated broad-acre crops
590 in an Australian semi-arid climate zone, *Environmental Earth Sciences*, 73, 449-465, 2015.

591 Wang, C.-Y., Wang, J.-N., Wang, X.-F., Luo, D.-L., Wei, Y.-Q., Cui, X., Wu, N., and Bagaria, P.:
592 Phenological Changes in Alpine Grasslands and Their Influencing Factors in Seasonally Frozen Ground
593 Regions Across the Three Parallel Rivers Region, Qinghai-Tibet Plateau, *Frontiers in Earth Science*, 9,
594 10.3389/feart.2021.797928, 2022.

595 Wang, S., Grant, R., Verseghy, D., and Black, T.: Modelling plant carbon and nitrogen dynamics of a
596 boreal aspen forest in CLASS—the Canadian Land Surface Scheme, *Ecological Modelling*, 142, 135-
597 154, 2001.

598 Wang, Y., Yao, G., Zuo, Y., and Wu, Q.: Implications of global carbon governance for corporate carbon



599 emissions reduction, *Frontiers in Environmental Science*, 11, 3, 2023a.

600 Wang, Y., Xiao, J., Ma, Y., Ding, J., Chen, X., Ding, Z., and Luo, Y.: Persistent and enhanced carbon
601 sequestration capacity of alpine grasslands on Earth's Third Pole, *Science Advances*, 9,
602 eade6875, doi:10.1126/sciadv.ade6875, 2023b.

603 Wang, Y., Xiao, J., Ma, Y., Luo, Y., Hu, Z., Li, F., Li, Y., Gu, L., Li, Z., and Yuan, L.: Carbon fluxes and
604 environmental controls across different alpine grassland types on the Tibetan Plateau, *Agricultural and
605 Forest Meteorology*, 311, 108694, 2021.

606 Wu, T., Ma, W., Wu, X., Li, R., Qiao, Y., Li, X., Yue, G., Zhu, X., and Ni, J.: Weakening of carbon sink
607 on the Qinghai–Tibet Plateau, *Geoderma*, 412, 115707, <https://doi.org/10.1016/j.geoderma.2022.115707>,
608 2022.

609 Y, W. Z., Y, L. Z., K, D. S., L, F. M., S, L. Y., M, L. S., N, W. S., H, M. C., X, M. T., and Y, C.: Evolution
610 of ecological patterns and its driving factors on Qinghai-Tibet Plateau over the past 40 years, *Acta
611 Ecologica Sinica*, 42, 8941-8952, 2022.

612 Yasin, A., Niu, B., Chen, Z., Hu, Y., Yang, X., Li, Y., Zhang, G., Li, F., and Hou, W.: Effect of warming
613 on the carbon flux of the alpine wetland on the Qinghai-Tibet Plateau, *Frontiers in Earth Science*, 10,
614 10.3389/feart.2022.935641, 2022.

615 Yu, Y.: Double-order system construction of China's climate change legislation under the dual carbon
616 goals, *China Population Resources and Environment*, 32, 89-96, 2022.

617 Yuanyuan, Z., Wanze, Z., Xiangyang, S., and Zhaoyong, H.: Carbon dioxide flux characteristics in an
618 *Abies fabri* mature forest on Gongga Mountain, Sichuan, China, *Acta Ecologica Sinica*, 38, 6125-6135,
619 2018.

620 Zhang, J., Lin, H., Li, S., Yang, E., Ding, Y., Bai, Y., and Zhou, Y.: Accurate gas extraction (AGE) under
621 the dual-carbon background: Green low-carbon development pathway and prospect, *Journal of Cleaner
622 Production*, 134372, 2022.

623

624